Quantifying the Signal-to-Noise Ratio of Silicon-Embedded Sensors for Mechanomyography

Silva J.[1], Chau T.[2], Naumann S.[2]

Departamento de Ingeniería Biomédica, Universidad Iberoamericana, México D. F., México.[1]
Rehabilitation Engineering Department, Bloorview MacMillan Children's Centre, Toronto, On. Canada.[2]
Institute of Biomaterials and Biomedical Engineering, University of Toronto, Toronto, On. Canada.[2]

Abstract. Experiments consisted of systematic measurements of the signal-to-noise ratio (SNR) of signals acquired from a mechanical stimulator, using silicon-embedded accelerometers. The objective of using the latter was to determine the combination of embedding properties which provide the highest SNR for mechanomyography (MMG) signal recording. Variations in silicon hardness and geometry were tested. Two important conclusions can be derived from the experiments: (1) It is possible to acquire MMG signals using silicon-embedded sensors; and (2) The embedded sensor's performance is affected by changes in the geometry of the embedding. The intended application of this study is the use of soft silicon suction sockets with embedded sensors as a more comfortable and functional alternative to current hard-socket powered prostheses for below-elbow amputees currently using electromyography as the control signal(s).

INTRODUCTION

Mechanomyography.

Mechanomyography (MMG)[1] is the epidermal measurement of the mechanical activity ("muscular sound") of contracting muscles. This phenomenon is a superficial summation of propagated motor unit twitches, and shape changes in muscular fibres during voluntary contractions [2]. It has been consistently stated that the MMG signal amplitude can be related to muscle strength in non-fatiguing contractions at fractions of maximum voluntary contraction (MVC) [1-6]. Previous studies show that most of the power of the MMG signal is located in the 0-45Hz bandwidth [1-5]. Furthermore, no significant frequency components have been reported beyond 100Hz for arm muscles. Muscle mechanical activity has been measured and recorded with piezoelectric microphones [3], condenser microphones [6], [7] and accelerometers [7], [8]. In order to filter out external "noise", some researchers have developed different methods to isolate the recording site. Courteville et al. (1998) used a complex fixing method to couple a microphone and a silicon support[2] to a foam armband. They used a silicon membrane to convert the displacement of the skin due to the muscle vibration into pressure waves for detection by microphone [6]. Goldenberg et al. (1991) reported the use of surgical cement for fixing a microphone to the skin over the ADM muscle of the subject's dominant hand [5].

Previous Theoretical Analysis.

A theoretical study showed that the fundamental oscillation frequency of the MMG decreases as the mass of the transducer increases [9]. Since this study is formulated on the basis of an ideal situation where the mass of the sensor is uniformly distributed along the muscle surface, it provides valuable information about the expected influence of the silicon-embedded sensor on the signal itself. On the other hand, Barry et al. (1986) suggested that muscle-molded transducers would increase the SNR in MMG measurements [10].

MMG & Prosthesis Control.

Although MMG signals have been described and studied for many years, they have never been used for practical prosthesis control. Barry et al. (1986) demonstrated that reliable control signals can be obtained from muscular mechanical activity, having tested a MMG-based control system to open and close a prosthetic hand [10]. While soft silicon suction sockets are a more comfortable and functional alternative for powered prostheses, sensor attachment issues have delayed their practical use [11]. Research on MMG as alternative channels for prosthesis control may cement the union between silicon sleeves and powered prostheses.

MATERIALS & METHODS

Preparation of Samples.

Three types of silicon with different hardness values (shores 20A, 35A and 65A) were chosen to prepare fifteen samples (five samples for each silicon type) of silicon-embedded sensors using BU-7135 accelero-meters from Emkay Innovative Products. Table 1 shows the dimensions of the samples for each silicon type. An initial silicon layer was placed on a flat surface before curing. The wired accelerometer was placed over the

[1] Term suggested by Orizio (1993) [1]
[2] Silicon RTV 1556

Table. 1. Embedding Properties of the Prepared Samples.

Sample No.	T_{TL} [mm]	T_{BL} [mm]
1	3.0	1.0
2	2.0	1.0
3	1.0	1.0
4	2.0	2.0
5	2.0	3.0

NOTE: All the samples were 32mm. width by 42mm. length.

silicon layer, this initial silicon layer constituted the bottom layer (BL) of the embedding. A second silicon layer, the top layer (TL), was placed over both the first layer and the sensor. The whole system was then cut down to its final dimensions. Finally, the sample was placed into an oven for the silicon to cure. Figure 1 shows a detailed diagram of the samples.

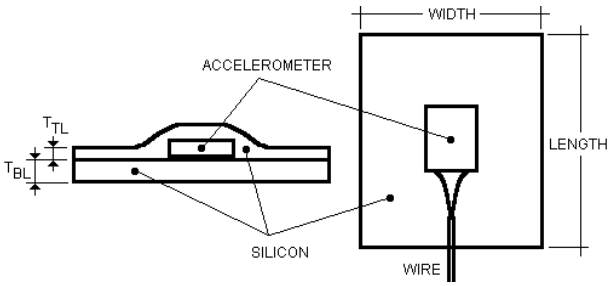

Fig. 1. Schematic diagram of the silicon-embedded accelerometers prepared. "T_{TL}" stands for Top Layer Thickness, "T_{BL}" stands for Bottom Layer Thickness.

Stimulus Generation.

A mechanical stimulator based on a WM-R57A card-type speaker from Panasonic (Figure 2), was used to transmit vibrations to the prepared samples. The "signal" was a pre-defined vibration pattern with no frequency components beyond 100Hz. The peak frequency (20 Hz) amplitude was approximately the same value as that of previously reported MMG signals (0.3 m/s^2) [7]. "Noise" consisted of a uniformly distributed random signal whose maximum amplitude was 15% of the "signal" peak amplitude. Both signals were generated electronically with a PC 16-bit soundcard using the MATLAB® environment.

Test Methodology

Two different stimuli were separately applied to each sample, one being a pure noise signal and the other, a vibration signal with additive noise. In order to determine the effect of contact surface changes on SNR,

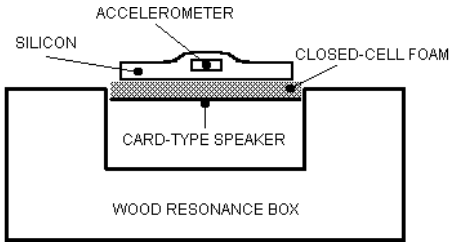

Fig. 2. Schematic diagram of the mechanical stimulator. Samples were placed over a closed-cell foam to assure physical contact.

two more sets of recordings were acquired after cutting down each dimension (width and length) by a 10mm decrement. The three surfaces tested were: 32x42mm, 22x32mm, and 12x22mm (width and length respectively). Root-mean-square (RMS) values of voltages obtained from the sensors were automatically calculated and stored for further analysis. Data from transducers were acquired through a pair of LM 386 audio amplifiers using a PC 16-bit soundcard. Two additional measurements with non-embedded transducers were used as control references for the experiments. From the RMS values obtained, we calculated the SNR of the sample using equation (1).

$$SNR = 10\log\left[\left(\frac{RMS_{SIGNAL+NOISE}}{RMS_{NOISE}} - 1\right)^2\right] \qquad (1)$$

Analysis & Validation Tests.

Forty repeated measurements for each sample (including the control) were recorded. The Lilliefors test for normality [12] was applied to the SNR data of each sample. Since some data did not follow a normal distribution, we used the Wilcoxon-Mann-Whitney rank sum one-sided test to determine whether or not the SNR values obtained for a certain combination of variables were higher than those of the non-embedded sensors. To test the hypothesis of independence between SNR and the other variables, the data were first organized into sensor groups. A sensor group is defined as a collection of samples which differ in only one variable (silicon type, top layer thickness, bottom layer thickness, or surface area). Subsequently, we constructed a contingency table with the observed frequencies of increasing, decreasing or non-monotonic trends in SNR. A Monte-Carlo simulation with 10^6 groups of random numbers provided the expected frequencies under the null hypothesis. A χ^2 test for goodness-of-fit was used to test the null hypothesis that there was no monotonic relationship between the SNR and the other variables. Finally, an adjusted residuals matrix [13] was computed to determine which types of

trends were significantly different from the expected values. For all statistical tests, a 5% significance level (α=0.05) was used

RESULTS

Table 2 shows the mean values of the SNR obtained for the hardest silicone type (shore 65A). Similar tables were obtained for each of the two remaining silicone types. In the shaded columns, the samples are denoted as x.y, where x is the sample number in Table 1, and y identifies the surface area, with y=1 signifying the largest surface. The Control (non-embedded) sample is included for comparison. Note that most of the SNR values for the embedded samples are higher than the ones obtained for the non-embedded samples.

Table. 2. Mean values of SNR obtained for the hardest silicon type (shore 65A)

Sample No.	SNR [dB]	Sample No.	SNR [dB]	Sample No.	SNR [dB]
Control	16.0	Control	16.0	Control	16.0
1.1	13.6	1.2	25.9	1.3	22.2
2.1	8.3	2.2	19.8	2.3	20.4
3.1	16.5	3.2	17.3	3.3	17.1
4.1	12.4	4.2	28.3	4.3	20.6
5.1	16.9	5.2	23.2	5.3	26.0

Table 3 shows the rank sum values (RSV) obtained for the samples reported in Table 2. The values that are significantly higher than the control at a 0.05 level of significance (RSV < 82) are highlighted in bold.

From the Monte-Carlo simulation we obtained probability values of 0.16, 0.16 and 0.66 for the probabilities of increasing, decreasing and non-monotonic trends, respectively. From the χ^2 test, we determined that SNR is dependent on the bottom layer thickness, top layer thickness, contact surface area and silicon hardness.

Table. 3. Rank sum values obtained for samples reported on Table 2. Significant differences are highlighted in bold.

Sample No.	RSV	Sample No.	RSV	Sample No.	RSV
1.1	155	1.2	**55**	1.3	**55**
2.1	155	2.2	**55**	2.3	**55**
3.1	**55**	3.2	**55**	3.3	**65•**
4.1	155	4.2	**55**	4.3	**55**
5.1	**55**	5.2	**55**	5.3	**55**

All values of $p << 0.05$
• $p = 0.025$

Finally, from residual analysis, the significant trends in the above dependencies were as follows:

The SNR increased as:

1. the bottom layer thickness increased.
2. the top layer thickness increased.
3. the contact surface area decreased.
4. the hardness of the silicon decreased.

CONCLUSIONS

Although the results suggest statistically significant trends, further experiments are needed to determine the exact nature of these dependencies. For example, in the case of contact surface area measurements, there may have been a mechanical damping effect exclusively due to the stimulator characteristics. This effect would not be present in real MMG measurements. Furthermore, the propagation of the MMG signals through the tissues may differ from the propagation of the vibration signal through the closed-cell foam (Figure 2).

Two main conclusions can be derived from the above results.

1. It is possible to record MMG signals using silicon-embedded sensors without appreciable loss of SNR.
2. Each embedded sensor performance is dependent on the geometry and silicon hardness of the embedding.

The demonstration of the feasibility to record MMG signals with silicon-embedded sensors is a required step towards the development of MMG-based control systems for soft silicon socket powered prosthesis.

ACKNOWLEDGEMENTS

The authors would like to acknowledge the support of the Bloorview MacMillan Children's Foundation.

REFERENCES

[1] C Orizio, "Muscle sound: Bases for the introduction of a mechanomyographic signal in muscle studies," *Critical Reviews in Biomedical Engineering*, vol. 21, no. 3, pp. 201–243, 1993.

[2] C Orizio, D Liberati, C Locatelli, D De Grandis, and A Veicsteinas, "Surface mechanomyogram reflects muscle fibres twitches summation," *Journal of Biomechanics*, vol. 29, no. 4, pp. 475–481, 1996.

[3] C Orizio, R Perini, B Diemont, M Maranzana Figini, and A Veicsteinas, "Spectral analysis of muscular sound during isometric contraction of

biceps brachii," *Journal of Applied Physiology*, vol. 68, no. 2, pp. 508–512, 1990.

[4] M Ouamer, M Boiteux, M Petitejean, L Travens, and A Salès, "Acoustic myography during voluntary isometric contraction reveals non-propagative lateral vibration," *Journal Biomechanics*, vol. 32, no. 12, pp. 1279–1285, 1991.

[5] MS Goldenberg, HJ Yack, FJ Cerny, and HW Burton, "Acoustic myography as an indicator of force during sustained contractions of a small hand muscle," *Journal of Applied Physiology*, vol. 70, no. 1, pp. 87–91, 1991.

[6] A Courteville, T Gharbi, and JY Cornu, "MMG measurement: A high-sensitivity microphone-based sensor for clinical use," *IEEE Transactions on Biomedical Engineering*, vol. 45, no. 2, pp. 145–150, 1998.

[7] M Watakabe, K Mita K Akataki, and Y Itoh, "Mechanical behaviour of condenser microphone in mechanomyography," *Medical & Biological Engineering & Computing*, vol. 39, no. 2, pp. 195–201, 2001.

[8] YT Zhang, C Basil, R Mandayam, and G Douglas, "A comparative study of simultaneous vibromyography and electromyography with active human quadriceps," *IEEE Transactions on Biomedical Engineering*, vol. 39, no. 10, pp. 1045–1052, 1992.

[9] LQ Zhao, YT Zhang, W Herzog, and DF Yuan, "A theoretical study of muscle vibrations: The influence of transducer mass on vibromyographic signals," in *Proceedings of the 20th Canadian Medical and Biological Engineering Society Conference*, 1994.

[10] DT Barry, JA Leonard, AJ Gitter, and RD Ball, "Acoustic myography as a control signal for an externally powered prosthesis," *Archives of Physical and Medical Rehabilitation*, vol. 67, no. 4, pp. 267–269, 1986.

[11] TAZK Gaber, CM Gardner, and SGB Kirker, "Silicone roll-on suspension for upper limb prosthesis: User's views," *Prosthetics and Orthotics International*, vol. 25, no. 2, pp. 113–118, 2001.

[12] WJ Conover, "Practical Nonparametric Statistics", John Wiley & Sons, 3rd edition, 1999.

[13] R Christensen, "Log-linear models", Springer-Verlag, 1990.